Lipid nanoparticle-mediated co-delivery of siRNA and paclitaxel for efficient SLC3A2 gene silencing in pancreatic cancer cells

Dilip Kumar R[*], S T Girisha, Samyami DP

Department of Microbiology and Biotechnology, Jnana Bharathi Campus, Bangalore University, Bangalore, Karnataka, India
*Corresponding author: E-mail: dilipkumar051994@gmail.com

Abstract

Paclitaxel, a widely used anticancer drug, stabilizes microtubules and induces apoptosis; however, its efficacy is often limited by drug resistance and poor tumor specificity. To overcome these limitations, we developed a lipid nanoparticle (LNPs) for the co-delivery of siRNA targeting the *SLC3A2* gene and paclitaxel. LNPs were formulated using DOTAP, DSPC, cholesterol, and PEG2000-DSPE in a molar ratio of 40:10:38.5:1.5. These lipid mixtures were combined with aqueous siRNA solutions at volume ratios of 1:5 and 1:10. Paclitaxel (25 μM) was subsequently incorporated via an ethanolic solution, and encapsulation efficiency was evaluated. The resulting paclitaxel-LNP-siRNA complexes were transfected into Mia PaCa-2 pancreatic cancer cells. Gene silencing efficacy was assessed using qPCR, western blotting, and confocal laser scanning microscopy. The paclitaxel-LNP-siRNA complexes exhibited a high encapsulation efficiency of 96.42% and demonstrated stability for over 30 days. qPCR analysis revealed a 93% reduction in *SLC3A2* gene expression, while western blotting showed an 82.3% decrease in protein levels. Confocal imaging confirmed successful transfection and gene silencing, evidenced by reduced fluorescence intensity in treated cells. These findings highlight the promise of a dual-delivery system aimed at enhancing anticancer effects through the combination of gene silencing and chemotherapy in pancreatic ductal adenocarcinoma.

1.INTRODUCTION

Pancreatic ductal adenocarcinoma (PDAC) is among the most lethal malignancies worldwide, currently ranked as the fourth leading cause of cancer-related deaths in developed nations (National Center for Chronic Disease Prevention and Health Promotion, 2022). Epidemiological projections suggest that PDAC will become the second leading cause of cancer mortality by 2030 (Rahib et al., 2014). Its aggressive nature, poor prognosis, and resistance to conventional therapies underscore the urgent need for novel and effective treatment strategies (Bugazia et al., 2024; Kokkinos et al., 2020). Among emerging approaches, RNA interference (RNAi)-based gene silencing has shown considerable promise in targeting oncogenic pathways in PDAC (Mansoori et al., 2014). Small interfering RNAs (siRNAs) can be designed to silence specific genes, including those encoding tumor-promoting proteins that are challenging to inhibit using traditional small molecules or monoclonal antibodies (Tatiparti et al., 2017; Zuckerman et al., 2015).

In this study, we targeted the SLC3A2 gene, which encodes the CD98 heavy chain (CD98hc)—a protein highly overexpressed in PDAC and involved in tumor cell proliferation, migration, and metabolic reprogramming. SLC3A2 functions as a chaperone for LAT1 (SLC7A5) and xCT (SLC7A11), regulating amino acid transport and oxidative stress response (Bianconi et al., 2022; Xia et al., 2022). Its overexpression is associated with tumor aggressiveness and therapeutic resistance, making it a compelling target for RNAi-based therapies (Badgley et al., 2020).

Despite the therapeutic potential of siRNAs, their clinical application is limited by rapid enzymatic degradation, poor systemic stability, and inefficient cellular uptake due to their hydrophilic nature and negative charge (Tatiparti et al., 2017; Zuckerman et al., 2015). Nanotechnology has emerged as a promising solution to these limitations (McCarroll et al., 2014). Nanoparticles (NPs) can protect siRNAs from enzymatic breakdown, enhance their cellular uptake, and enable controlled intracellular release. However, optimal siRNA delivery requires nanoparticles with a mild positive charge to bind negatively charged siRNA electrostatically, while maintaining near-neutral surface charge to improve tumor penetration and reduce toxicity—especially important in the dense extracellular matrix environment of PDAC (Jyotsana et al., 2019; Nguyen et al., 2017; Xin et al., 2017). The size, charge, and surface chemistry of nanoparticles play critical roles in determining their biological performance, biodistribution, and safety profile (Beddoes et al., 2015).

Although multiple nanoparticle-based platforms have been developed for the co-delivery of paclitaxel (PTX) and siRNA to enhance anticancer efficacy, no studies to date have specifically targeted SLC3A2. Recent innovations include bioinspired, tumor-homing nanoparticles coated with cancer cell membranes for the co-delivery of PTX and E7-targeted siRNA in cervical cancer, resulting in enhanced tumor targeting and immune evasion (Tran et al., 2017; Xu et al., 2020). Another study introduced PEG-detachable, pH-responsive polymeric nanoparticles for the co-delivery of PTX and VEGF siRNA in breast cancer, demonstrating synergistic tumor suppression by targeting angiogenesis (Jin et al., 2021). Additionally, multifunctional FeCo-PEI-PLA-PEG nanoparticles have shown effective co-delivery of siRNA and PTX to drug-resistant breast cancer cells, enhancing cytotoxicity while minimizing off-target effects (Nasab et al., 2021). These advances highlight the growing potential of nanoparticle-mediated co-delivery strategies for overcoming resistance and improving therapeutic outcomes in cancer.

In this context, our study employs lipid nanoparticles (LNPs) composed of 1,2-dioleoyl-3-trimethylammonium-propane (DOTAP), distearoylphosphatidylcholine (DSPC), cholesterol, and polyethylene glycol 2000-distearoylphosphatidylethanolamine (PEG2000-DSPE). DOTAP, a cationic lipid, facilitates electrostatic complexation with siRNA, ensuring high encapsulation efficiency. DSPC contributes to membrane stability and structural integrity. Cholesterol enhances bilayer stability and promotes cellular uptake, while PEG2000-DSPE prolongs systemic circulation by reducing opsonization and

reticuloendothelial clearance (Akbaba et al., 2017; Terada et al., 2021).

To the best of our knowledge, there are no previous studies evaluating the synergistic effects of paclitaxel co-delivery alongside SLC3A2 gene silencing. Therefore, this research aims to synthesize and evaluate LNP-siRNA (SLC3A2)-PTX complexes in Mia PaCa-2 pancreatic cancer cells. Key evaluations include complexation efficiency, nanoparticle stability, and gene scilencing efficiency assessed via quantitative RT-PCR, Western blotting, and Confocal Laser Scanning Microscopy (CLSM). By confirming SLC3A2 suppression at both mRNA and protein levels, this study provides valuable insights into the therapeutic potential of LNP-mediated co-delivery systems for improving PDAC treatment.

2. MATERIALS AND METHODS

2.1 Synthesis and characterization of LNP-siRNA complex: LNP were prepared by dissolving DOTAP, DSPC, Cholesterol and PEG2000-DSPE in ethanol at distinct molar ratios 40:10:38.5:1.5 as described by Wan *et al* (2014). siRNA targeting SLc3A2 (sequence: CAAGAACCAGAAGGAUGAU dTdT), was added to the lipid mixture (1:5 and 1:10 ratio) to make LNP-siRNA systems (Jin et al., 2021). The LNP-siRNA integrated complexes (LNP-siRNA) were dialyzed and centrifuged to collect the stable LNP-siRNA and were stored at 4°C (Yu et al., 2012). These complexes were characterised using Transmission Electron Microscopy (TEM) and Dynamic Light Scattering (DLS) to determine their morphology, size, and surface characteristics (Park et al., 2023).

Table 1: Primers used for real-time PCR

	CTGACTTCAACAGCGACACC
GAPDH	GTGGTCCAGGGGTCTTACTC
	CCTTGTGCTGGGTCCAATTC
SLc3A2	AGTTCTCACCCCGGTAGTTG

2.2 Study of siRNA Integrity
The complexation efficiency of siRNA integrity with drug was evaluated using a gel retardation assay. Samples were loaded onto a 1% agarose gel containing ethidium bromide and electrophoresis was performed. The bands were visualised under UV illumination, and band intensities were quantified using ImageJ software. The complexation efficiency (%) was calculated using the formula: = (Intensity of naked siRNA – Sample Intensity) × 100/ naked siRNA intensity

2.3 Cell Culture and *in vitro* Transfection in Mia PaCa-2 Cells:
Mia PaCa-2 cells were maintained in DMEM supplemented with 10% FBS and 1% PenStrep at 37°C with 5% CO_2. Cells were trypsinized, resuspended in complete DMEM, and seeded at 250,000 cells/well in a 6-well plate. After 24 hours, when a partial monolayer formed, the medium was removed, and cells were washed with serum-free DMEM. Cells were transfected with LNP mixed with aqueous solution of siRNA (50μM) at ratios of 1:5 and 1:10, and Lipofectamine mixed with siRNA (positive control). 100 μL of each transfection mixture was added per well, for 6 wells plate each contain pre incubated 2.5 lakh cell, and cells were incubated at 37°C with 5% CO_2 for 24 hours. Further, the PTX (25μM) was loaded with better-performing LNP-siRNA-complex (1:5 ratio). All combinations of LNP, LNP-siRNA complexes and PTX- LNP-siRNA complexes were transfected trice to target cells and their gene silencing efficiency for downregulating SLC3A2 was measured in two replicates to find reproducibility.

2.4 Gene Expression Analysis by qPCR
For gene expression analysis, after the transfection with different LNP systems or lipofectamine mixed with siRNA, total RNA was isolated, using Trizol reagent (Takara Bio, USA) following the manufacturer's protocol. RNA quantification was performed using Spectramax i3x (Molecular Devices, USA), and samples were stored at -20°C for further analysis. cDNA synthesis was carried out from 1 μg of total RNA using the Takara Bio RT-PCR kit, employing specific primers for SLC3A2 and GAPDH (Table 1). Real-time PCR (q-PCR) was conducted using the Bio-Rad CFX 384-well system. All reactions were performed three times in a 10-μl reaction volume. The expression level of genes was measured using the comparative Ct method.

2.5 Protein expression Analysis using Western blot
protein expression analysis, Mia PaCa-2 cells were transfected with different LNP systems or lipofectamine associated with siRNA. For protein analysis, 100 μg of total protein extracted from cell lysates was mixed with 5X loading dye, denatured at 98°C for 6 minutes, and separated on a 12% SDS-PAGE gel using Mini-Protean Tetra Cell (Bio-Rad). Proteins were transferred to a methanol-activated 0.45 μm PVDF (polyvinylidene fluoride) membrane using the Turbo Transblot system (Bio-Rad) for 10 minutes. The membrane was blocked with 5% BSA in tris-buffered saline with Tween-20 (TBST) for 1 hour at room temperature, followed by overnight incubation at 4°C with the primary antibodies (1:1000 dilution). After three TBST washes, the membrane was incubated with HRP-conjugated secondary antibody (1:5000 dilution) for 1 hour at room temperature,

washed, and developed using an ECL reagent system. SLC3A2 (Proteintech, 1:500), and GAPDH (Sigma-Aldrich, 1:500) were used as primary antibody, however, the secondary antibody was anti-rabbit IgG (Sigma-Aldrich, 1:5000). Protein bands were visualized using a ChemiDoc MP Imaging System (Bio-Rad) with a 40-second exposure.

2.6 Confocal laser scanning microscopy
MiaPaCa-2 cells were seeded onto Ibidi® μ-Slide 8 Well plates and incubated overnight for adherence. The cells were transfected with LNP-siRNA-PTX and untreated control for 24 hours at 37°C in a 5% CO_2 incubator. Following incubation, cells were washed three times with 1X PBS and fixed at -20°C for 10 minutes. The fixed cells were blocked with blocking buffer for 30 minutes at room temperature, followed by incubation with the primary antibody targeting SLC3A2 for 2 hours. After washing, cells were incubated with FITC-conjugated secondary antibody (Thermo Fisher, Cat# A-11035). Nuclei were counterstained with DAPI (Cat# 005VGMRL1 VNIR) for 5 minutes, and slides were visualized using a Leica confocal laser microscope as per the manufacturer's guidelines

3. RESULT AND DISCUSSION

Lipid nanoparticles (LNPs) containing pH-responsive ionizable cationic lipids are widely recognized for their efficiency in delivering and releasing siRNAs into cells. These amphiphilic lipids self-assemble with siRNA through electrostatic interactions under acidic conditions, enabling high encapsulation efficiency while maintaining a near-neutral surface charge at physiological pH—thereby reducing both toxicity and immunogenicity (Kokkinos et al., 2020).

3.1 Synthesis and characterization of nanoparticles
A novel lipid nanoparticle (LNP)-siRNA complex was synthesized using DOTAP, DSPC, cholesterol, and PEG2000-DSPE in a 40:10:38.5:1.5 ratio. Transmission electron microscopy (TEM) and dynamic light scattering (DLS) analyses confirmed that the resulting LNP-siRNA complexes were compact and spherical in shape. The diameters of the nanoparticles ranged from 220 nm to 300 nm, with an average diameter of 260 ± 7 nm, as shown in Fig. 1 (a). A similar study by Wang et al (2015) employed DOTAP, neutral lipids (cholesterol, DOPE), and DSPE-PEG2000 to develop a stable nanoparticle system (~260 nm) for siRNA delivery. The hydrodynamic size distribution of the LNP-siRNA complex was determined using DLS, as shown in Fig. 1(b), revealing an average size of 230 nm (Fig 1c). Zeta potential measurements were conducted to assess the colloidal stability of LNP, as shown in Figure 3b. The obtained value of 0.1 mV indicates a high level of cell stability. The stability of cationic solid lipid nanoparticles (cSLNs) against particle aggregation for up to 30 days was likely due to strong electrostatic repulsion among cationic particles (Rietwyk et al., 2017).
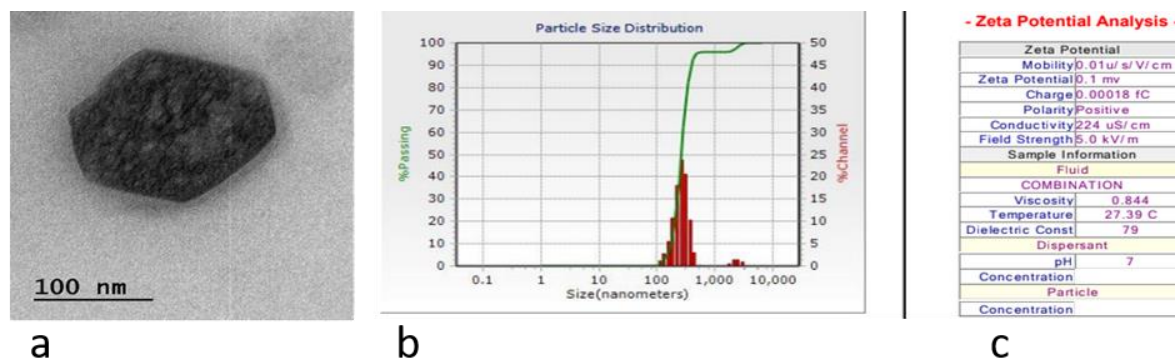

Figure 1: Characterization of Nanoparticles
(a)Transmission electron microscopic view of siRNA integrated Lipid Nanoparticle (b) DLS (c) Zetapotential

3.2 Study of siRNA Integrity
The stability and encapsulation efficiency of our LNP-siRNA complex highlight the importance of rational nanoparticle design in improving systemic biodistribution and therapeutic efficacy for targeted gene delivery in pancreatic cancer (Melamed et al., 2023; Taniuchi et al., 2019). Quantitative analysis of band intensities revealed a complexation efficiency of 96.42% LNP-siRNA (band intensity: 660.34), while both PTX integrated with LNP-siRNA (1:5) exhibited complete encapsulation (100%), and PTX-LNP-siRNA (1:10) exhibited 71.64% complexation efficiency due to the high concentration of siRNA. In contrast, the naked siRNA control showed a band intensity of 18,452.6, confirming its un-encapsulated state (Figure 2). These results suggest that the LNPs effectively protected siRNA from enzymatic degradation, ensuring its integrity during transfection. The incorporation of ionizable lipids has been shown to significantly improve siRNA integrity, as demonstrated by Lee et al. (2012) using DLin-KC2-DMA in prostate cancer and Jyotsana et al. (2019) using DLin-MC3-DMA in chronic myeloid leukemia.

3.3 Relative gene analysis of LNP-siRNA complexes
These initial assessment of the transfection efficiency of LNP, lipofectamine, and LNP mixed with entrapped siRNA at ratios of 1:5 and 1:10 using qPCR reported that the LNP-siRNA complex (1:5) achieved the highest gene silencing efficiency due to optimized nanoparticle uptake and siRNA release within the cells. It showed the most significant reduction in SLC3A2 gene expression, with a 0.21-fold downregulated relative expression, as shown in Figure 3 (a). The variability in actin expression across samples remained minimal, confirming the reliability of normalization in this study. Although, no similar study has been conducted, this suggests that LNP-siRNA (1:5) complexed with PTX could mitigate effects associated with high SLC3A2 expression, such as chemoresistance, metabolic adaptation, and enhanced survival.

We further investigated the impact of co-delivering paclitaxel with the LNP-siRNA complex, which resulted in the most pronounced suppression of gene and protein expression. This could be attributed to disrupted nutrient uptake and redox homeostasis, making cells more vulnerable to paclitaxel-induced apoptosis. On comparing the transfection efficiency of PTX-loaded LNP-siRNA complex with Lipofectamine, the PTX-LNP-siRNA complex showed the best results, with a 0.07-fold (93% decreased) downregulation of the relative expression of SLC3A2 normalized to the housekeeping gene, GAPDH (Figure 3 (b)). These findings align with previous studies reporting that paclitaxel priming enhances the delivery and transfection efficiency of lipid-siRNA complexes in pancreatic cancer models (Wang et al., 2014; Wong et al., 2014).

Table 2: Complexation efficiency of different drug-siRNA combinations

Concentration	Band intensity	Complexation efficiency (%)
LNP-siRNA	660.43	96.42
PTX-LNP-siRNA (1:5)	0	100
PTX-LNP-siRNA (1:10)	5231.47	71.64
Naked siRNA	18452.58	-

Figure 2: Agarose gel electrophoresis image of siRNA encapsulation in LNP

3.4 Protein Expression Analysis

Western blot analysis was performed to evaluate the expression levels of SLC3A2 protein in different treatments, with actin serving as the loading control. The results demonstrated notable variations in protein expression under different conditions. In the first set of experiments, lipofectamine-siRNA treatment exhibited relative 0.53197 protein expression of SLC3A2 expression, whereas LNP-siRNA (1:5) showed a significantly reduced expression (0.3490). Interestingly, LNP-siRNA (1:10) exhibited the highest SLC3A2 expression (0.77), indicating a dose-dependent response (Figure 4a and b).

In the second set, LNPs exhibited expression similar to that of the control, whereas lipofectamine treatment resulted in a notable decrease (0.4816). PTX-loaded LNPs and LNP-siRNA complexes further reduced SLC3A2 protein expression, with LNP-siRNA-drug complexes demonstrating the most significant, 87.3% suppression (0.1867. These findings suggest that the siRNA-LNP formulation effectively downregulates SLC3A2 expression, with paclitaxel-loaded complexes exhibiting enhanced silencing efficiency (Figure 4 c, d). Notably, the dose-dependent response observed with the LNP-siRNA (1:5) complex indicates that optimizing siRNA concentration is crucial for maximizing silencing efficiency. This could be attributed to disrupted nutrient uptake and redox homeostasis, making cells more vulnerable to paclitaxel-induced apoptosis (Laroui et al., 2014; Wang et al., 2014).
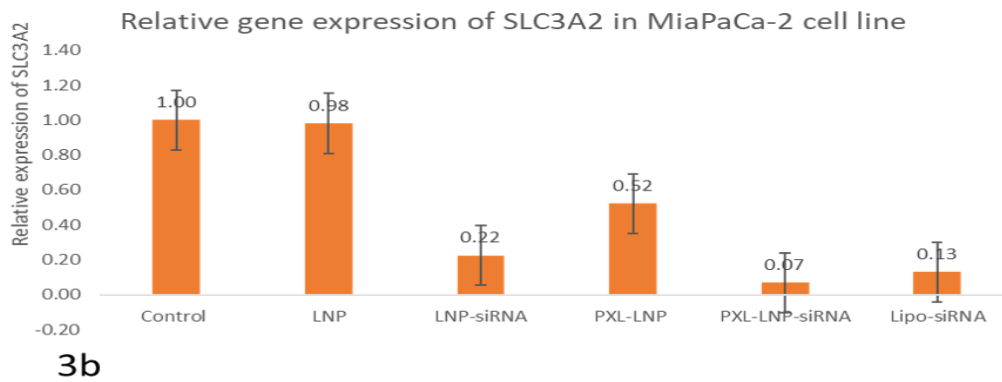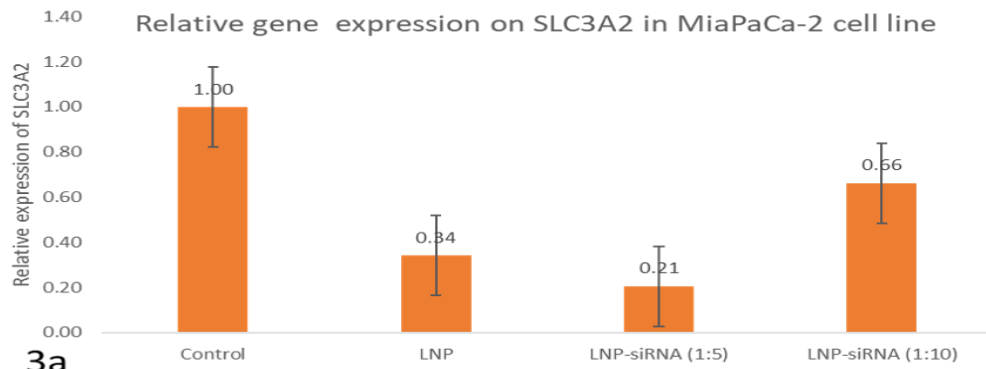
3a

3b

Figure 3: Relative gene expression analysis of SLC3A2 in MiaPaCa-2 cell lines

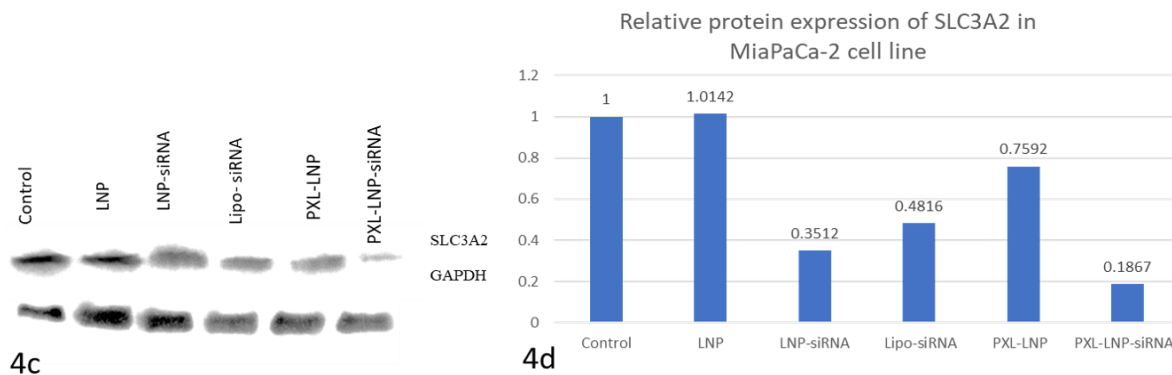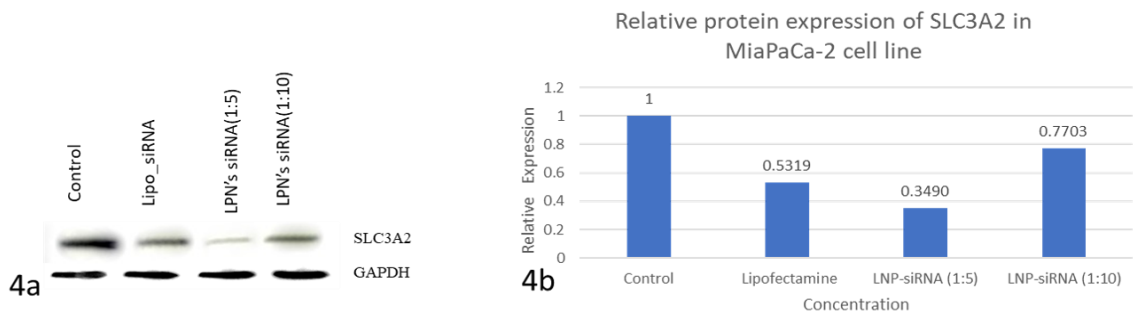

4a

4b

4c

4d

Figure 4: Protein expression analysis of SLC3A2 on MiaPaCa 2 cell line transfected with different ratios of lipid Nanoparticles

3.5 Confocal Microscopy Analysis of siRNA-LNP Transfection in MiaPaCa-2 Cells

Confocal microscopy images illustrate the expression and localization of SLC3A2 protein following LNP-siRNA transfection in MiaPaCa-2 cells. FITC-tagged images showed green fluorescence, and DAPI-stained images highlighted nuclear staining, confirming the presence of intact cells. However, merged FITC and DAPI staining demonstrated the co-localization of SLC3A2 protein and nuclear staining. We noted that control cells did not have any toxic effect on cells, and FITC-tagged antibody bound to the expressed SLC3A2 protein, showing high fluorescence intensity in DAPI nuclei, which appeared blue, indicating the presence of intact cells, consistent with previous studies.

In contrast, LNP-siRNA-PTX was effectively taken up by MiaPaCa-2 cells after 1.5 h of exposure (Figure 5). No further increase in fluorescence signal was observed. The reduced green fluorescence confirmed effective gene silencing by the LNP-siRNA complexes. Cells transfected with LNP-siRNA-paclitaxel showed greater suppression of SLC3A2 expression, compared to control groups, supporting the RNA silencing efficiency of the optimized formulation. Hence, confocal laser scanning microscopy supported successful transfection, showing decreased FITC fluorescence in treated cells, indicating effective SLC3A2 silencing. Significant suppression of LNP-siRNA-paclitaxel treated group confirms the synergistic effect of gene silencing and chemotherapy. Similar outcomes were observed by Laroui et al. with CD98 siRNA/PEI-loaded nanoparticles, and by Wang et al. (2015) with paclitaxel-loaded lipid-siRNA systems.
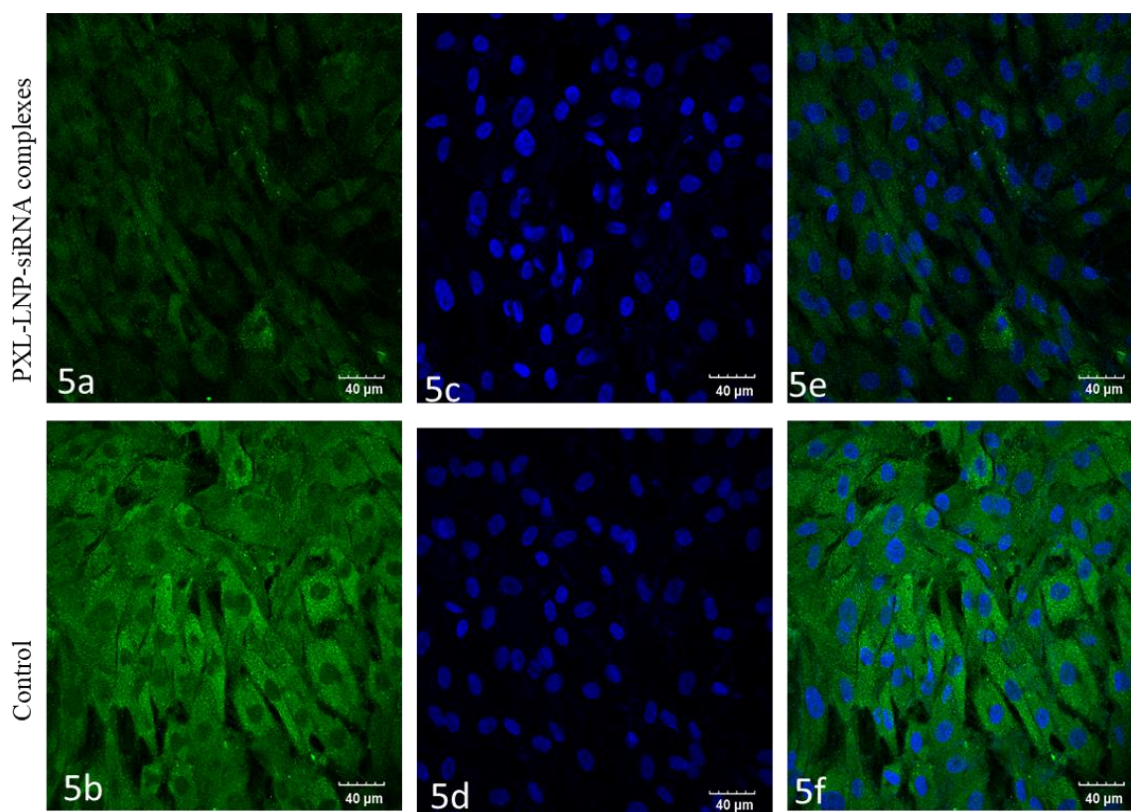

Figure 5: Confocal laser scanning microscopic view of cells after intracellular release of siRNA and drug from Paclitaxel-LNP-siRNA complexes

4. CONCLUSIONS AND FUTURE PROSPECTS

The findings of the present study underscore the potential of LNP-mediated siRNA delivery as a viable therapeutic strategy for PDAC. Furthermore, the results validated the feasibility of paclitaxel-loaded LNP-siRNA complexes for targeted gene silencing in pancreatic cancer. The study indicated that drug-loaded nanoparticle-based siRNA delivery enhanced gene silencing efficiency owing to the synergistic effects of the drug and siRNA. However, future studies should focus on *in vivo* evaluations to assess the biodistribution, pharmacokinetics, and therapeutic efficacy. Additionally, optimizing LNP formulations to enhance tumor penetration and minimize immunogenicity is critical for clinical translation.

ABBREVIATIONS

LNP- Lipid nanoparticles
LNP- siRNA integrated with Cationic lipid nanoparticles
PTX-LNP- paclitaxel loaded into LNP
PTX-LNP-siRNA complexes- Paclitaxel-loaded to siRNA integrated Cationic lipid nanoparticles

REFERENCES

- Akbaba, H., Karagöz, U., Selamet, Y. and Kantarcı, A.G. 2017. Synthesis and characterization of cationic lipid-coated magnetic nanoparticles using multiple emulsions as microreactors. Journal of Magnetism and Magnetic Materials, 426: 518–524.
- Badgley, M.A., Kremer, D.M., Maurer, H.C., DelGiorno, K.E., Lee, H.J., Purohit, V., et al. 2020. Cysteine depletion induces pancreatic tumor ferroptosis in mice. Science, 368(6486): 85-89.
- Beddoes, C.M., Case, C.P. and Briscoe, W.H. 2015. Understanding nanoparticle cellular entry: a physicochemical perspective. Advances in Colloid and Interface Science, 218: 48–68.
- Bianconi, D., Fabian, E., Herac, M., Kieler, M., Thaler, J., Prager, G., et al. 2022. Expression of CD98hc in pancreatic cancer and its role in cancer cell behavior. Journal of Cancer, 13: 2271–2280.
- Bugazia, D., Al-Najjar, E., Esmail, A., Abdelrahim, S., Abboud, K., Abdelrahim, A., et al. 2024. Pancreatic ductal adenocarcinoma: the latest on diagnosis, molecular profiling, and systemic treatments. Frontiers in Oncology, 14: 1386699.
- Jin, M., Hou, Y., Quan, X., Chen, L., Gao, Z. and Huang, W. 2021. Smart polymeric nanoparticles with pH-responsive and PEG-detachable properties: co-delivery of paclitaxel and VEGF siRNA for synergistic breast cancer therapy in mice. International Journal of Nanomedicine, 16: 5479–5494.
- Jyotsana, N., Sharma, A., Chaturvedi, A., Budida, R., Scherr, M., Kuchenbauer, F., et al. 2019. Lipid nanoparticle-mediated siRNA delivery for safe targeting of human CML in vivo. Annals of Hematology, 98(8): 1905–1918.
- Kang, Y.H. and Park, J.W. 2023. Preparation, characterization, and stability of lipid nanoparticles including unsaturated lipids. Tenside Surfactants Detergents, 60(6): 594-598.
- Kokkinos, J., Ignacio, R.M., Sharbeen, G., Boyer, C., Gonzales-Aloy, E., Goldstein, D., et al. 2020. Targeting the undruggable in pancreatic cancer using nano-based gene silencing drugs. Biomaterials, 240: 119742.
- Laroui, H., Geem, D., Xiao, B., Viennois, E., Rakhya, P., Denning, T., et al. 2014. Targeting intestinal inflammation with CD98 siRNA/PEI-loaded nanoparticles. Molecular Therapy, 22(1): 69-80.
- Lee, H., Lytton-Jean, A.K., Chen, Y., Love, K.T., Park, A.I., Karagiannis, E.D., et al. 2012. Molecularly self-assembled nucleic acid nanoparticles for targeted in vivo siRNA delivery. Nature Nanotechnology, 7(6): 389–393.
- Mansoori, B., Sandoghchian Shotorbani, S. and Baradaran, B. 2014. RNA interference and its role in cancer therapy. Advanced Pharmaceutical Bulletin, 4(4): 313-321.
- McCarroll, J., Teo, J., Boyer, C., Goldstein, D., Kavallaris, M. and Phillips, P.A. 2014. Potential applications of nanotechnology for the diagnosis and treatment of pancreatic cancer. Frontiers in Physiology, 5: 2.
- Melamed, J.R., Yerneni, S.S., Arral, M.L., LoPresti, S.T., Chaudhary, N., Sehrawat, A., et al. 2023. Ionizable lipid nanoparticles deliver mRNA to pancreatic β cells via macrophage-mediated gene transfer. Science Advances, 9(4): 1444.
- Nasab, S.H., Amani, A., Ebrahimi, H.A. and Hamidi, A.A. 2021. Design and preparation of a new multi-targeted drug delivery system using multifunctional nanoparticles for co-delivery of siRNA and paclitaxel. Journal of Pharmaceutical Analysis, 11(2): 163–173.
- National Center for Chronic Disease Prevention and Health Promotion (U.S.), Division of Cancer Prevention and Control. 2022. An update on cancer deaths in the United States. Available from: https://stacks.cdc.gov/view/cdc/119728
- Nguyen, V.H. and Lee, B.J. 2017. Protein corona: a new approach for nanomedicine design. International Journal of Nanomedicine, 12: 3137–3151.
- Rahib, L., Smith, B.D., Aizenberg, R., Rosenzweig, A.B., Fleshman, J.M. and Matrisian, L.M. 2014. Projecting cancer incidence and deaths to 2030: the unexpected burden of thyroid, liver, and pancreas cancers in the United States. Cancer Research, 74: 2913-2921.
- Rietwyk, S. and Peer, D. 2017. Next-generation lipids in RNA interference therapeutics. ACS Nano, 11(8): 7572-7586.
- Tatiparti, K., Sau, S., Kashaw, S.K. and Iyer, A.K. 2017. siRNA delivery strategies: a comprehensive review of recent developments. Nanomaterials, 7(4).
- Taniuchi, K., Yawata, T., Tsuboi, M., Ueba, T. and Saibara, T. 2019. Efficient delivery of small interfering RNAs targeting particular mRNAs into pancreatic cancer cells inhibits invasiveness and metastasis of pancreatic tumors. Oncotarget, 10(30): 2869.
- Terada, T., Kulkarni, J.A., Huynh, A., Chen, S., van der Meel, R., Tam, Y.Y., et al. 2021. Characterization of lipid nanoparticles containing ionizable cationic lipids using design-of-experiments approach. Langmuir, 37(3): 1120-1128.
- Tran, B.N., Nguyen, H.T., Kim, J.O., Yong, C.S. and Nguyen, C.N. 2017. Combination of a chemopreventive agent and paclitaxel in CD44-targeted hybrid nanoparticles for breast cancer treatment. Archives of Pharmacal Research, 40: 1420-1432.
- Wang, J., Lu, Z., Yeung, B.Z., Wientjes, M.G., Cole, D.J. and Au, J.L. 2014. Tumor priming enhances siRNA delivery and transfection in intraperitoneal tumors. Journal of Controlled Release, 178: 79-85.
- Wang, J., Lu, Z., Wang, J., Cui, M., Yeung, B.Z., Cole, D.J. 2015. Paclitaxel tumor priming promotes delivery and transfection of intravenous lipid siRNA in pancreatic tumors. J Control Release. 216:103-110.
- Wong, M.H. 2014. Overcoming primary and acquired erlotinib resistance with EGFR and PI3K co-inhibition in pancreatic cancer. [Thesis], The University of Sydney.
- Xia, P. and Dubrovska, A. 2023. CD98 heavy chain as a prognostic biomarker and target for cancer treatment. Frontiers in Oncology, 13: 1251100.
- Xin, Y., Huang, M., Guo, W.W., Huang, Q., Zhang, L.Z. and Jiang, G. 2017. Nano-based delivery of RNAi in cancer therapy. Molecular Cancer, 16(1): 134.
- Xu, C., Liu, W., Hu, Y., Li, W. and Di, W. 2020. Bioinspired tumor-homing nanoplatform for co-delivery of paclitaxel and siRNA-E7 to HPV-related cervical malignancies for synergistic therapy. Theranostics, 10(7): 3325.
- Yu, Y,H., Kim. E., Park, D.E., Shim, G., Lee, S., Kim, Y.B., Kim, C.W., Oh, Y,K. (2012). Cationic solid lipid nanoparticles for co-delivery of paclitaxel and siRNA. European Journal of Pharmaceutics and Biopharmaceutics. 80(2):268-73.
- Zuckerman, J.E. and Davis, M.E. 2015. Clinical experiences with systemically administered siRNA-based therapeutics in cancer. Nature Reviews Drug Discovery, 14(12): 843-856